Push or Pull? The Light-Weight Architecture of the *Daphnia pulex* Carapace is Adapted to Withstand Tension, Not Compression

Sebastian Kruppert,[1]* Martin Horstmann,[1] Linda C. Weiss,[1,2] Clemens F. Schaber,[3] Stanislav N. Gorb,[3] and Ralph Tollrian[1]

[1]*Department of Animal Ecology, Evolution and Biodiversity, Ruhr-University Bochum, Universitätsstraße 150, Bochum, 44780, Germany*
[2]*Environmental Genomics Group, School of Biosciences, University of Birmingham, Birmingham, B15 2TT, UK*
[3]*Department of Functional Morphology and Biomechanics, Christian-Albrechts-Universität Zu Kiel, Am Botanischen Garten 9, Kiel, 24118, Germany*

ABSTRACT *Daphnia* (Crustacea, Cladocera) are well known for their ability to form morphological adaptations to defend against predators. In addition to spines and helmets, the carapace itself is a protective structure encapsulating the main body, but not the head. It is formed by a double layer of the integument interconnected by small pillars and hemolymphatic space in between. A second function of the carapace is respiration, which is performed through its proximal integument. The interconnecting pillars were previously described as providing higher mechanical stability against compressive forces. Following this hypothesis, we analyzed the carapace structure of *D. pulex* using histochemistry in combination with light and electron microscopy. We found the distal integument of the carapace to be significantly thicker than the proximal. The pillars appear fibrous with slim waists and broad, sometimes branched bases where they meet the integument layers. The fibrous structure and the slim-waisted shape of the pillars indicate a high capacity for withstanding tensile rather than compressive forces. In conclusion they are more ligaments than pillars. Therefore, we measured the hemolymphatic gauge pressure in *D. longicephala* and indeed found the hemocoel to have a pressure above ambient. Our results offer a new mechanistic explanation of the high rigidity of the daphniid carapace, which is probably the result of a light-weight construction consisting of two integuments bound together by ligaments and inflated by a hydrostatic hyper-pressure in the hemocoel. J. Morphol. 000:000–000, 2016. © 2016 Wiley Periodicals, Inc.

KEY WORDS: *Daphnia*; carapace; cuticle; pillars; light-weight construction

INTRODUCTION

The freshwater crustacean *Daphnia* has been of special interest for ecological research due to its key position in limnetic ecosystems. As the dominant zooplankton in freshwater ecosystems, it controls algal growth and serves as a food source for numerous invertebrate and vertebrate predators. Its short generation time and parthenogenetic mode of reproduction allow rapid colonization of lakes and ponds (Louette and De Meester, 2004). Yet, one of the most remarkable features of *Daphnia* is its ability to develop inducible defenses (reviewed in Tollrian and Dodson, 1999). These defenses thwart predation and increase survival chances (Grant and Bayly, 1981). To date, three types of inducible defenses have been described: i) behavioral defenses, including the popular example of diel vertical migration (Lampert, 1989); ii) life-history shifts, where somatic growth is traded for reproduction (Stibor, 1992; Taylor and Gabriel, 1992; Stibor and Lüning, 1994); and iii) morphological defenses. A range of adaptive morphological traits has been observed, including impressive crests in *Daphnia longicephala* HEBERT (Barry, 2000), long helmets in *Daphnia lumholtzi* G. O. SARS (Tollrian, 1994) and minute 'neckteeth' in *Daphnia pulex* DE GEER (Krueger and Dodson, 1981). In general, defensive traits are described as 'anti-lock-and-key' systems; during attack the prey's defense structure interferes with, or even blocks, the predator's mouthparts (Dodson, 1974), obstructing capture or ingestion. While this hypothesis may hold true for the obvious defense structures such as crests or spines, it appears less feasible for unimposing structures like the

Sebastian Kruppert and Martin Horstmann contributed equally to this manuscript.

*Correspondence to: Sebastian Kruppert, Department of Animal Ecology, Evolution and Biodiversity, Ruhr-University Bochum, Universitätsstraße 150, Bochum 44780, Germany.
E-mail: sebastian.kruppert@rub.de

Received 19 February 2016; Revised 2 June 2016;
Accepted 25 June 2016.

Published online 00 Month 2016 in
Wiley Online Library (wileyonlinelibrary.com).
DOI 10.1002/jmor.20577

neckteeth developed by *D. pulex*. Aside from adaptive morphologies *D. pulex* possesses a more general defense against mechanical impact, that is, a body armor formed by a bivalved carapace. The carapace is an evagination of the integument extending from the cephalic region (Fryer, 1996). The crustacean integument is arranged in layers (Stevenson, 1985). The most distal layer, termed epicuticle, is very thin and delimits the body from the surrounding medium. The adjacent layer is the procuticle, generally subdivided into the exocuticle and endocuticle in crustaceans, although these are indistinguishable in daphniids. These cuticle layers are secreted by the underlying epidermal cells (Stevenson, 1985), which are interconnected by the extracellular matrix. As the daphniid's carapace is an integumental fold, it possesses two integumental layers piled in a reverse complement manner (Halcrow, 1976). The space between the layers is filled with hemolymph (Anderson, 1933; Halcrow, 1976), and they are interconnected by irregularly dispersed structures, so-called pillars (Anderson, 1933; Halcrow, 1976; Fryer, 1996). Laforsch et al. (2004) showed that the adapted neckteeth morphotype is also characterized by a fortification of the whole body armor as well as a measured increase in pillar diameter. This led to the hypothesis that pillars were responsible for the observed carapace fortification (Laforsch et al., 2004). The mechanism by which these pillars could provide cuticle reinforcement was not determined. However, this information is crucial to understand the protective effect of the hidden morphological defenses in *D. pulex*.

In order to analyze the protective capacity of the carapace structure, we aimed to determine how the pillars are linked to the integuments of the carapace and describe the integument's morphology in detail. We used different imaging techniques [light microscopy (LM), transmission and scanning electron microscopy (SEM)] to analyze the morphology of both the proximal and distal integuments of the carapace and the interconnecting pillars. We found that the structure of the pillars is characterized by fibrillae with extensively branched roots extending into the proximal and distal integument.

METHODS

Experimental Organisms

Daphnia pulex (Leydig, 1860), clone R9 (originating from Canada) and *D. longicephala* (Hebert, 1977), clone LP1 (from Lara Pond, Australia) were cultured under constant conditions with a day:night cycle of 16:8 h at 20°C ± 0.1°C in a climate chamber. Both species were cultured in 1 l glass beakers containing charcoal-filtered tap water and fed ad libitum with the algae *Scenedesmus obliquus*.

In Vivo LM

Six adult *D. pulex* were analyzed using LM to assess the appearance of pillars at the dorsal keel. The animals were transferred to an object slide (Menzel GmbH & Co KG, Braunschweig, Germany) with a drop of water. Images were taken with a Colorview III camera (Olympus Soft Imaging Systems, Münster, Germany) mounted on an SZX16 dissecting microscope (Olympus, Hamburg, Germany) using the software Cell'D (Olympus, Hamburg, Germany).

Whole Mounts Stained with Hematoxylin and Eosin

The hematoxylin and eosin (HE) stain is usually employed as a routine method to differentiate between tissues, cells or cell compartments with acidophilic and basophilic properties. Hematoxylin stains nucleic acids (predominantly located within nuclei) blue, while eosin stains cytoplasm and connective tissue red. The specimens were fixed in 4% formaldehyde diluted from 37% formaldehyde (J.T. Baker, Germany) with phosphate buffered saline (PBS; 0.1 mol l^{-1}, pH 7.4). Staining of whole mount preparations (15 specimens of *D. pulex*) were performed according to the manufacturer's protocol (Thermo Scientific, Waltham, United States of America, provided as SHANDON™ instant-dyes). Briefly, *D. pulex* were rinsed three times in PBS (pH 7.4, 0.1 mol l^{-1}) and incubated in Instant Hematoxylin (Thermo Scientific™ Shandon™ Instant Hematoxylin, Thermo Fisher Scientific Inc., Waltham, MA) for 3 min, then rinsed for 2 s with hydrochloric acid (HCl; 0.1 N) until differentiation. The process was terminated by rinsing the samples in deionized water for 1 min. Samples were transferred into Instant Eosin (Thermo Scientific™ Shandon™ Instant Eosin, Thermo Fisher Scientific Inc., Waltham, MA) for 3 min. Immediately after staining, the specimens were dehydrated in an ascending ethanol series: 80% ethanol (2 × 2 min), 95% ethanol (3 × 2 min), 100% isopropanol (2 × 2 min) and 100% Roti-Histol (3 × 3 min) (Roti®-Histol, Carl Roth GmbH & Co. KG, Karlsruhe, Germany). Finally, the samples were mounted and cover-slipped in Entellan (Entellan®, Merck KG aA, Darmstadt, Germany) on object slides (Menzel GmbH & Co KG, Braunschweig, Germany), using ringed sticky tape (Avery Zweckform; Valley, Germany; Weiss et al., 2012). LM was carried out using a Zeiss Axiovert (Zeiss, Oberkochen, Germany) with an XC10 monochrome camera (Olympus, Hamburg, Germany) and CellSens® digital imaging software (Olympus, Hamburg, Germany). The pillar density (no. of pillars per area) and base diameter were measured along a ventral-to-dorsal transect across a central region of the carapace (Fig. 1). Pillars were counted in squares of 100 × 100 μm along the transect and the diameter of their bases recorded. Due to inter-individual variation in body width, 6–8 squares were necessary to cover the entire transect. Squares were numbered 1–7, as this represented the average number of squares. Where more or less than seven squares were required, the squares numbers were multiplied by $n/7$ where n is the total number of squares, normalizing all squares to point numbers between one and seven. Division by body length was used to normalize the pillar base diameter.

Scanning Electron Microscopy

For SEM, the samples (19 *D. pulex*, second juvenile instar) were fixed in 70% ethanol and dried according to the standard procedure using hexamethyldisilazane (HMDS, Sigma-Aldrich, St. Louis, MO; Laforsch and Tollrian, 2000). Subsequently, they were mounted on aluminum blocks using 'Leit tabs' ('Conduction-Tab', Plano GmbH, Wetzlar, Germany). To visualize the interconnecting pillars, the dried carapace was fractured using fine dissection needles (euromex microscopes b.v., Arnhem, The Netherlands). Some of the fractured specimens did not have a clear breaking edge but the proximal integument was removed with the dissecting needle. The samples were sputter-coated with gold (Sputter Coater SCD 050, BALZER, 180 sec, 10,000 V) and visualized with an SEM (DSM 950, Zeiss, Oberkochen, Germany).

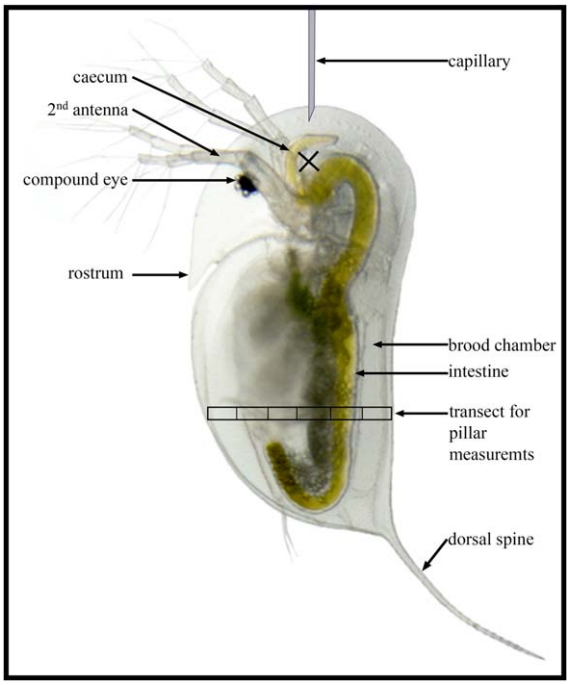

Fig. 1. *Daphnia longicephala*, overview image Illustrating the transect over which the pillar density and base diameter were determined (which is also the region of the cross-section shown in Fig. 3), and the area pierced for hemolymphatic gauge pressure measurements (black X).

Thin Sections

The specimens were fixed in 1% glutaraldehyde (VWR, Radnor, PA) buffered in PBS (0.1 mol l^{-1}, pH 7.4) overnight. After fixation, the samples (17 *D. pulex*, second juvenile instar) were rinsed in PBS 3 × 30 min and contrasted for 40 min with 2% osmium tetroxyde solution (Heraeus, Hanau, Germany). Samples were dehydrated in an ascending ethanol series of 50% (15 min), 70% (overnight), 90% (25 min), 100% (5 min) and 2 × 100% (30 min). Infiltration with Agar 100 (Agar Scientific, Essex, UK) was carried out according to the manufacturer's protocol. The resin was polymerized at 60°C for 48 h in a Teflon mould (Sigma-Aldrich Chemie GmbH, Munich, Germany). Specimens were positioned in an anterior–posterior direction in the moulds in order to produce cross sections. Blocks were trimmed and processed using an ultra-microtome (Reichert Jung Ultracut E, Leica Microsystems, Wetzlar, Germany), equipped with an glass-knife set to an angle of 7°. Sections with thicknesses of 1.5–3 μm were collected in a drop of water on a glass slide (VWR; Radnor, Pennsylvania) and dried on a heat plate (Medax, Neumünster, Germany) at 60°C for 15 min. The sections on the glass slides were stained with a drop of 0.1% toluidine blue staining solution (dissolved in deionized water). Excess dye was rinsed off with deionized water after 2 min. Images were taken with a XC10 monochrome digital camera (Olympus, Münster, Germany) attached to a Zeiss Axiovert (Zeiss, Oberkochen, Germany) LM and processed using CellSens® Digital Imaging Software (Olympus, Germany).

Ultra-Thin Sections and Scanning Transmission Electron Microscopy

Ultra-thin cross-sections (45–70 nm thick) of Agar 100 embedded specimens were also cut with the ultra-microtome using a diamond knife with a 2.5 mm edge (Diatome 45°, Diatome, Hatfield, PA) equipped with a water-filled 'boat' for collecting the sections, and set to an angle of 7°. Expansion of the floating sections was facilitated using xylol fumes from a wooden stick. The floating sections were transferred to copper grids with a mesh width ranging from 20 to 80 lines per cm (Stork Veco B.V., Eerbeek, Holland) by picking them up directly from the surface. Scanning transmission electron microscopy (STEM) of ultra-thin sections of 17 animals was conducted on a Zeiss Gemini (Zeiss Gemini Sigma VP, Zeiss, Oberkochen, Germany). The acceleration voltage was set to 20 kV and STEM detector was set to 'dark field segment mode', resulting in images comparable to dark field TEM.

Measurements of the thickness of the proximal and distal procuticle, the distance between the proximal and distal procuticle at the ventral and dorsal edge, as well as the middle region of the carapace and thickness of single pillar fibres were conducted using the software Zeiss SmartTiff (Version V02.01, Carl Zeiss Microscopy Limited, Cambridge, UK).

Hemolymphatic Gauge Pressure

The hemolymphatic gauge pressure measurements were performed in vivo using *D. longicephala*—taking advantage of their comparatively large size. Animals were fixed in a lateral position on an object slide with underwater adhesive (JBL 'Haru', Neuhofen, Germany). The pressure was measured in the head capsule in the near-vicinity of the caeca (Fig. 1). This region contains the largest volume in a *Daphnia*'s hemolymph system, thus facilitating precise penetration and measurement. We used an invasive blood pressure system, similar to those used in medical applications. A pressure transducer (Deltran® Disposable Pressure Transducer, Utah Medical Products, Inc., Midvale, UT) was connected to a glass capillary via a silicon tube, and additionally, also via silicon tubing, to a syringe (single-use, 5 ml; Amefa; Limburg, Germany) to remove excess air from the system. The capillary (Premium Standard Wall Borosilicate Capillary Glass, OD 1.5 mm, ID 0.86 mm, L 100 mm; Harvard Apparatus; Holliston, MA) was pulled with a micropipette puller (P-97 Flaming/Brown Micropipette Puller; Sutter Instrument; Novato, CA), with a tip-diameter of approximately 15 ± 1 μm. The transducer was linked to a data recording device including a digitizing system and a signal amplifier (Biopac, Model MP100A-CE; BIOPAC Systems Inc., Santa Barbara, CA), which subsequently transmitted the data to a computer. For the measurements, animals were quickly fixed and transferred into a water-filled petri-dish placed under a dissection microscope (SZX12, Olympus, Germany), this was performed carefully to avoid harm to the organism. The capillary was positioned with a micromanipulator (Prior Scientific, Rockland, ME) at an angle of approximately 30° to the surface. A rapid forward movement of the capillary was used for penetration. Once the capillary tip pierced the integument its position was maintained for 5–10 s to ensure stable pressure measurement and then it was extracted. Pressure recording began prior to penetration and continued at 200 measurements per second until extraction of the capillary was complete. In total, the hemolymphatic gauge pressure was measured in 39 animals.

RESULTS

Morphology of the Carapace and Distribution of the Pillars

The histological analysis of the daphniid carapace focused on the dorsal keel, because it exhibits comparatively large pillars, which can be observed with LM (Fig. 2A). Images of HE-stained animals revealed the pillars of the dorsal keel region to be slim-waisted and connected to the proximal and distal integument via broad branched bases, which could also be observed in vivo (Fig. 2B). Particle motion in the space between distal and proximal integument indicated hemolymph flow.

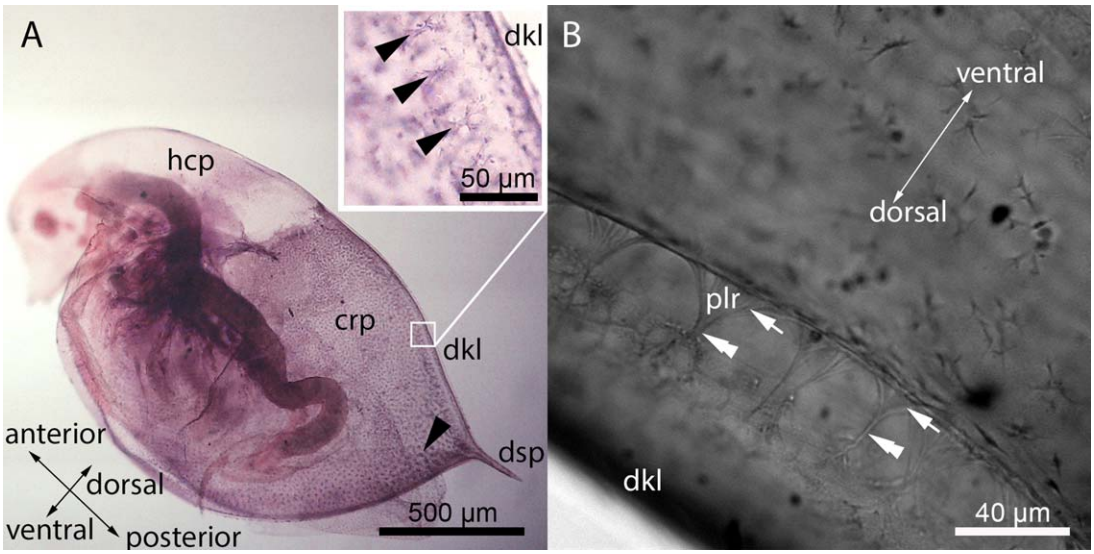

Fig. 2. Overview of the daphniid carapace and its structure A. *Daphnia pulex*, adult individual hematoxylin-eosin stained. The head region (hcp) is covered by a single layer integument. The body behind the head is protected by the carapace (crp), which prolongates into the dorsal spine (dsp). In the carapace, pillars are visible as spots. The inset shows a region of the dorsal keel (dkl). The arrowheads point to single pillars. **B**. In vivo observation of an adult *D. pulex* at the dorsal keel. Pillars (plr) have a base on either side (arrows), sometimes branching into 4–6 roots. The bases converge into the pillar waist (double arrowheads) connecting the proximal and distal integument.

Our HE-stains differentiated the nuclei (blue) and the extracellular matrix (pink). Figure 2A displays a representative whole mount preparation of *D. pulex* with clearly contrasted pillars distributed irregularly across the carapace. The animal's head is covered by a single integumental layer forming the head capsule. The body and the filtering legs are enclosed by a bivalved carapace, which is an evagination of the cephalic region (Olesen, 2013). Dorsally the carapace is fused to a keel that extends into a spine. The ventral side remains unfused, leaving a gap, the so-called ventral cleft, crucial for food intake and respiration. The ventral cleft serves as an opening allowing continuous water current by articulated limb movement. This continuous stream allows the uptake of food particles and gas exchange. The distance between proximal and distal integument is wider at the ventral margin and the dorsal keel in relation to the central region (Fig. 3A). The bases of the pillars varied in density and diameter (Figs. 2A and 3B,C). Pillar bases in the central carapace region had narrow diameters, whereas those near the ventral cleft and dorsal keel were wider and branched into four to six roots (Fig. 2B). In these distal regions the number of pillars per 10,000 μm^2 was lower than in the central region (Fig. 3C).

The toluidine blue stained cross-sections displayed the epidermis in high contrast, as well as clearly contrasting the pillars and the cuticle layers. The cross-sections also revealed slim-waisted pillars with broad bases branching into roots that attached to the integuments (Fig. 4A).

Similarly, SEM images also displayed pillars with slim waists and broad bases that appeared branched at the integuments (Fig. 4B). Furthermore, the SEM samples clearly displayed the pillars to be fibrous structures, interconnected with the extracellular matrix (Fig. 4B). The extracellular matrix was particularly visible in the electron microscopic images (Fig. 4B,C), allowing a 3D-impression of its fibrous structure (Fig. 4C).

Due to the thinness of the proximal integument, the epicuticle and procuticle could only be distinguished in the high magnification of STEM-images (Fig. 5A,C). Similarly, the proximal epidermis was thinner than the distal and barely visible with LM (Figs. 4A,B and 5A).

Ultrastructure of the Pillars

The broad bases and the extracellular matrix were clearly observable in SEM samples where the proximal integument of the carapace had been mechanically removed (Fig. 4C).

STEM and SEM micrographs showed the pillars to be interconnected with the extracellular matrix (Figs. 4B and 5A). We found the distal integument to be much thicker than the proximal one. The mean thickness of the *D. pulex* distal procuticle was 0.982 ± 0.334 µm [± standard deviation (SD)], compared with 0.581 ± 0.195 µm for the proximal procuticle. This difference is statistically highly significant ($P < 0.005$, *t*-test, *t*-value 4.28, 17 specimens each). The underlying epidermis generally followed similar proportions. The procuticle clearly showed a laminated structure (Figs. 4B and 5A).

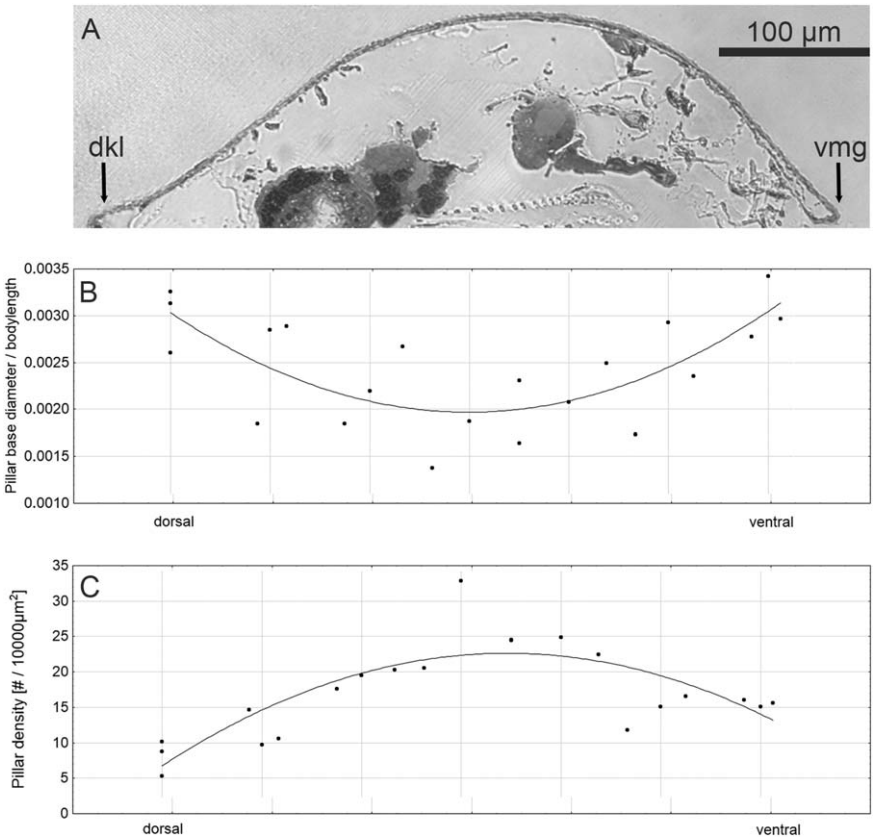

Fig. 3. *Daphnia pulex*, pillar density and base diameter along a ventral-dorsal transect in the central region of the carapace. **A**. Cross section of *D. pulex* displaying one lateral half of the carapace between the dorsal keel (dkl) and the ventral margin (vmg). **B**. Body length normalized pillar base diameter along a ventral-dorsal transect (data from three animals). **C**. Average pillar density (pillars/10,000 µm^2) along a ventral to dorsal transect (data from three animals).

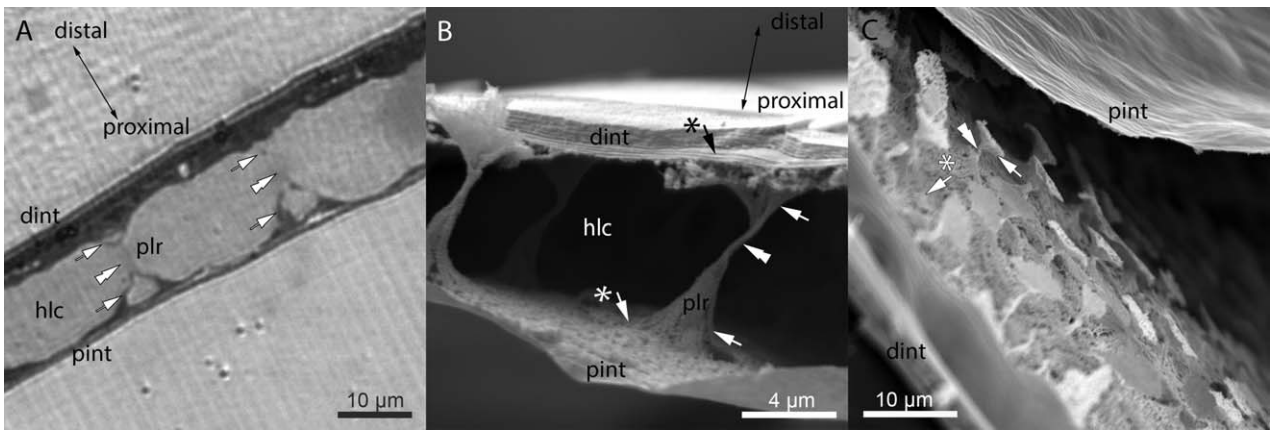

Fig. 4. *Daphnia pulex*, carapace structure and pillar details. **A**. Light microscopic micrograph of a toluidine blue stained section of the proximal (pint) and distal (dint) carapace integument connected by the pillars (plr) bridging the hemolymphatic chamber (hlc) in between. Arrows point to pillar bases, double arrowheads to pillar waists. **B**. B. Scanning electron micrograph of a pillar of a fractured *D. pulex* carapace connecting the proximal (pint) and the distal (dint) integumental layers. The white arrows point to the pillar bases, the white double arrowhead to the pillar waist, the white arrow with an asterisk to the extracellular matrix, and the black arrow with an asterisk to the laminar structure of the procuticle. **C**. Scanning electron micrograph of the *D. pulex* carapace. The proximal integument (pint) is peeled off revealing the pillar bases (white arrow) with widely branched roots. The white double arrowhead indicates a pillar waist and the white arrow with an asterisk the extracellular matrix.

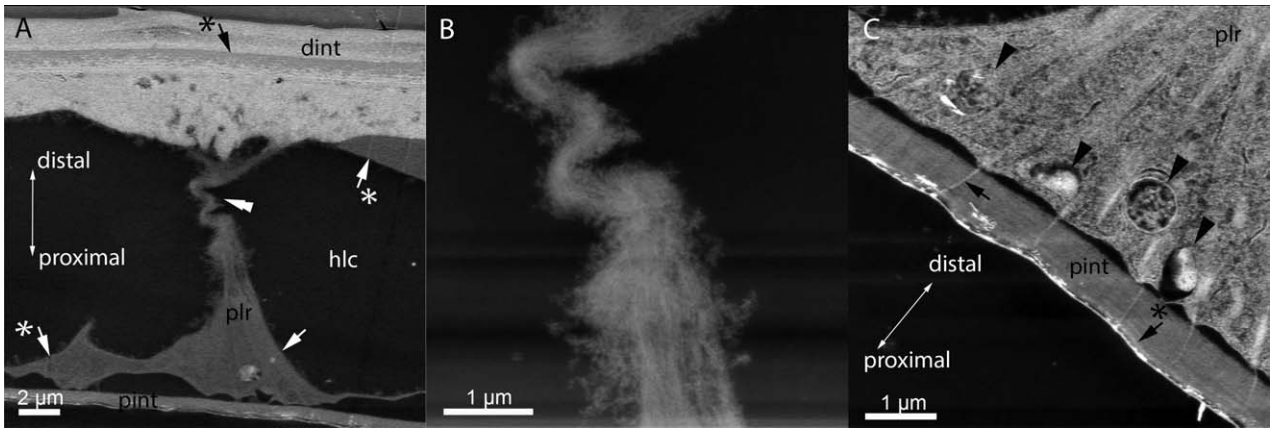

Fig. 5. *Daphnia pulex*, STEM images of pillar details. **A**. STEM image of a cross-section of a pillar anchoring the proximal and distal integument. The proximal procuticle (pint) is notably thinner than the distal (dint), which shows a laminar structure (black arrow with an asterisk). The white arrow points to the pillar base, the white double arrowhead to the pillar waist and the white arrow with an asterisk to the extracellular matrix. **B**. Higher magnification STEM image of the central waist of the pillar displayed in A. Note the tightly arranged fiber bundles. **C**. STEM micrograph displaying the pillar base. Cell organelles, nucleus and mitochondrion (black arrowheads) are located within the pillar base. Several fibers connect the pillar's base with the procuticle (pint). These intracuticular fibers extend from within the pillar (plr) and anchor it, thoroughly pervading the procuticle (black arrow). The black arrow with an asterisk indicates the laminar structure of the procuticle.

STEM-images showed that the pillars possess a fibrous structure (Fig. 5B), supporting the SEM observations. The single pillar fibers are tightly arranged into fiber bundles and have an average thickness of 14.67 ± 2.49 nm (mean $\pm$ SD, $n = 8$). Many of the visualized pillars were found to be collapsed (Fig. 5B), which may be an artifact of the preparation procedure. The fibrous structures of the pillars span through the epidermis and connect to the procuticle via fine insertions. Furthermore, a variety of cell organelles including mitochondria and nuclei were visible in some pillar bases (Fig. 5C).

Hemolymphatic Pressure

The median gauge pressure of *D. longicephala*'s hemolymph was 3.12 mbar (Fig. 6). The measurements showed high variance and ranged from a minimum of 0.08 mbar up to 9.73 mbar. However, all measurements showed a positive gauge pressure in the hemolymphatic chamber.

DISCUSSION

We analyzed the integument of the *Daphnia* carapace in order to evaluate the contribution of interconnecting pillars to the carapace's capability to

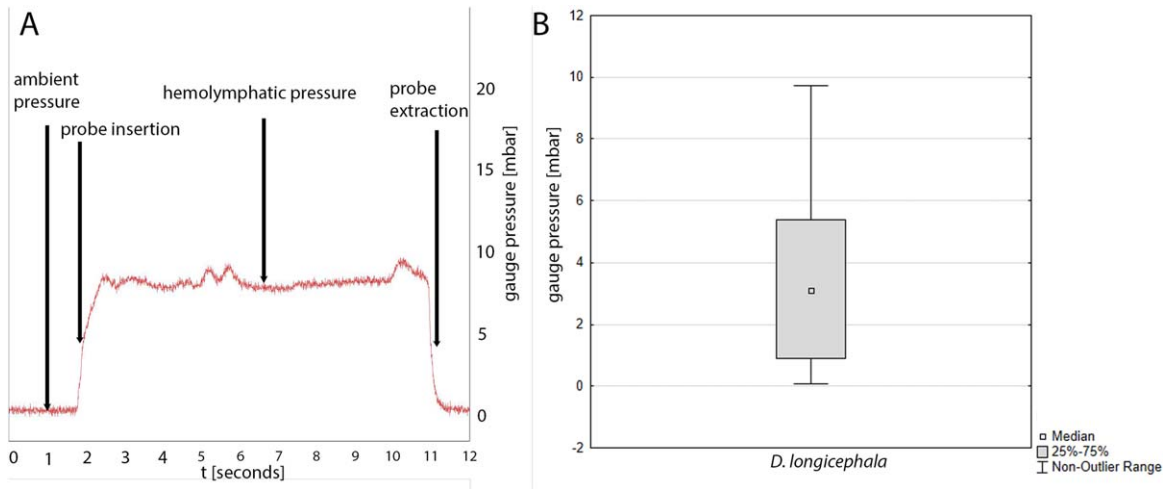

Fig. 6. Measurements of the hemolymphatic gauge pressure. **A**. Example measurement profile of the hemolymphatic gauge pressure of one individual animal. **B**. Boxplot of the hemolymphatic gauge pressure measurements.

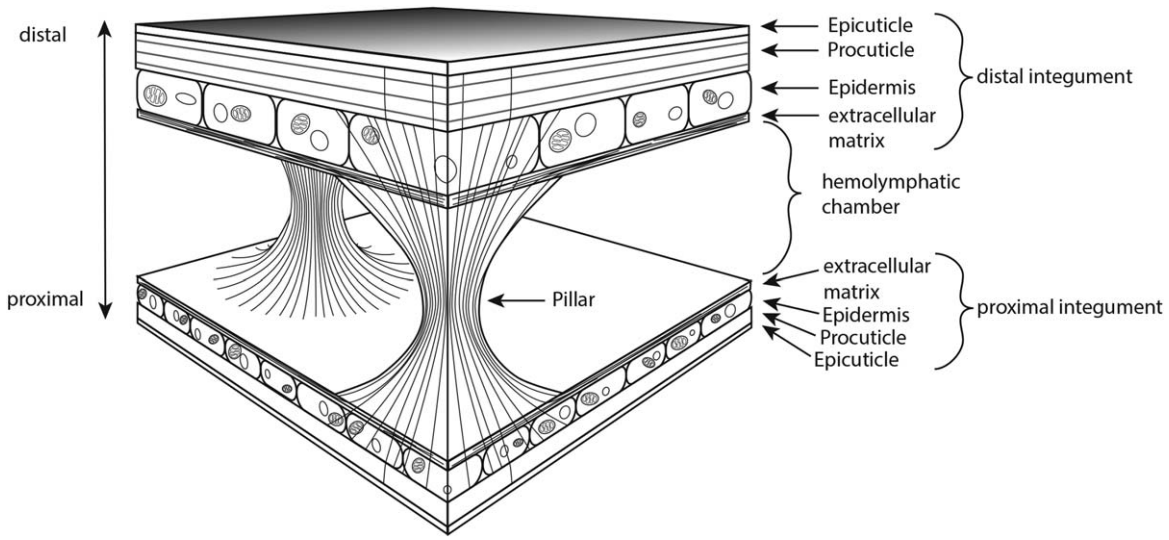

Fig. 7. Schematic drawing of the *Daphnia* carapace structure. The carapace is composed of two integumental layers in reverse complement manner and interconnected by pillars.

withstand compressive forces. We found the proximal integument to be significantly thinner than the distal, which is in accordance with earlier descriptions (Anderson, 1933; Halcrow, 1976; Fryer, 1996; Pirow et al., 1999a,b). The interconnecting pillars appeared fibrous, slim-waisted and tightly attached to the epidermis and anchored in the procuticle via intercuticular fibers. This observation is in contrast to their hypothesized function as load bearing structures (Anderson, 1933; Laforsch et al., 2004) and rather indicates the capability to withstand tensile forces.

Carapace Proximal and Distal Integument Structure

We observed that the distal integument was clearly distinguishable into the epicuticle, multilayered procuticle, epidermis and extracellular matrix (Figs. 4A,B, 5A and 7) confirming earlier studies (Halcrow, 1976; Stevenson, 1985). The thickness of the distal integument probably reflects a higher risk of perforation by predators' mouthparts. Furthermore, the relative thinness of the proximal integument reflects its contribution to daphniid respiration, that is, the thin integument facilitates oxygen uptake from the permanent water current in the filtering chamber produced by the beating thoracopods (Fryer, 1991; Pirow et al., 1999a,b).

Interconnecting Pillars

Our results show that the pillars connecting the distal and proximal integuments within *Daphnia* carapaces are slim-waisted with broad, branched bases. These findings were independent of the preparation method used (in vivo, Fig. 2B; resin embedding, Figs. 4A and 5A; or HMDS drying, Fig. 4B,C) and are in agreement with the description reported by Anderson (1933), who sketched them with thin centers but assigned them a supporting function. Our investigations revealed that the pillars consist of single fibers, packed together to form the characteristic pillar shape (Fig. 5B). Anderson assumed that these pillars are chitinous (Anderson, 1933) but our stains indicate that they originate from the connective tissue of the extracellular matrix, since the HE stained the pillars a reddish color. In addition, the pillar fibers share characteristics with intermediate filaments. Their thickness is on average 14.66 nm, which lies within the range of intermediate filament thickness (10–15 nm; between microfilaments (5–8 nm) and microtubules (20–30 nm)). Furthermore, due to preparation the fibers often appeared bent in the waist region of the pillars and thus seem to be resistant against shear forces. Intermediate filaments are known for being far more resistant against shear forces than microfilaments and microtubules (Janmey, 1991). We found that some of the fibers reached through the epidermis, anchoring the pillar in the procuticle (Fig. 5C). These are analogous to the anchoring fibers in arthropods that reach through the epidermis and into the procuticle to attach muscle (Bitsch and Bitsch, 2002). Znidaršič et al. (2012)showed for isopods, that these fibers even reach through the new procuticle and anchor in the old procuticle just before molting. In *Daphnia*, such attachment fibers to the exoskeleton were described for muscles by Schulz and Kennedy (Schultz and Kennedy, 1977) and in association with pillars by Halcrow (Halcrow, 1976).

Pillar Function

Laforsch et al. (2004) described the carapace as a light-weight construction capable of

withstanding mechanical impact and compressive forces. If that were the case, then the supporting elements should be composed of solid columns without any distinct thin weak points. Chen et al. (2015) analyzed pillar structures in the elytra of *Dorcus titanus* (Insecta) and showed that they are optimized for uptake of compressive forces. Morphologically, these pillars are solid columns with broad bases and no waists. Their internal structure is characterized by chitin fibers, reinforced by a sclerous-protein matrix that continuously merges from the procuticle into the pillar. This continuous transition from the rigid procuticle fiber-matrix into the pillars reinforces the weak points of this pillar type, that is, the pillar-procuticle contact area. In contrast to the elytra pillars the *Daphnia* pillars have broad bases but slim waists and are most likely composed of intermediate filaments. These filaments continuously extend into the extracellular matrix and are additionally anchored vertically in the procuticle. The vertical anchoring translates tension forces, acting on the pillars, to the procuticle in proximal direction which is its optimal load angle. The pillars' broad bases offer a larger contact surface between integuments and pillars, allowing a higher potential to withstand tensile forces due to the distribution of forces over a larger area. The slim waists do not negatively affect the capability to withstand tensile forces because the material properties, diameter and number of fibers are more important than the shape in which they are composited (Ottani et al., 2001). In fact the broad bases and slim waists mirror the mushroom-shape of adhesive structures in, for example, *Chrysomelidae* (Insecta, Coleoptera). These adhesive structures were found to be capable of taking high tensile loads before losing contact (Carbone et al., 2011; Heepe and Gorb, 2012). In general, biological structures responsible for taking up or even storing tensile forces are comparatively thin and fibrous, for example, tendons or roots (Mattheck 1998). Tensile forces imposed on the integumental layers could result from hemolymph that fills the space between the two integumental layers of the carapace. This can be observed in insect wing expansion during adult emergence. Insect wings also consist of two integuments that are closely interconnected via microtubule rich cells, each anchored by fibers in the procuticle (Nardi and Ujhelyi, 2001). For expansion, hemolymph is pumped between the layers. If the hemolymphatic pressure in *Daphnia* is higher than that of the surrounding medium (i.e., the water body), similar stabilizing elements are necessary to prevent the carapace integuments from drifting apart. Such gauge pressure would contribute to the animal's resistibility against mechanical impact by providing a hydrostatic force that works against such impact (comparable to the increase in an air bed's stiffness with increasing gauge pressure). During a local impact caused by a predatory attack the loaded pillars would buckle (not break) and the stress would be distributed over a larger area via an increase of the hemolymphatic pressure, resulting in tensile forces acting on the pillars in the surrounding areas. In addition to the protective function of the carapace, the pillars are also relevant for respiration. While the hemolymphatic chamber between the two layers would collapse in case of negative gauge pressure it would expand without the pillars in case of positive gauge pressure. Thus, the pillars' resistibility against tension forces is crucial for the known functions of the carapace, that is, protection and respiration.

The median hemolymphatic gauge pressure measured directly in live *D. longicephala* was 3.12 mbar (Fig. 6). Measuring the hemolymphatic gauge pressure in *D. pulex* would have been challenging with our experimental setup due to their smaller size. Although the variation was high, all measurements showed a positive gauge pressure and thus proved the hemolymphatic pressure to be higher than the pressure of the surrounding medium. Data variability might result from the invasiveness of the method, where sealed connection cannot be assured and capillary penetration depth cannot be kept constant per individual trial. Furthermore, the animals might have suffered from different stress levels, during the in vivo procedure, which influences the hemolymphatic pressure. The differences in pillar density and base diameter between central regions of the carapace and the dorsal keel as well as the ventral margin could be the result of a trade-off between the strength of the ties between the integument layers and hemolymphatic flow resistance. At both the dorsal keel and ventral margin, the hemolymphatic current is higher than in the central region (Pirow et al., 1999a,b) and the integuments are separated by a wider gap. The reduced number of pillars might be a concession to the hemolymphatic current, enabling a better flow, and compensated by a larger connection (pillar base) for each interconnection. In conclusion, the pillars operate against tensile forces resulting from hemolymphatic pressure, rather than countering superimposed compressive forces. In order to reflect the pillars' function, we suggest using the term 'ligaments' in analogy to the structures that interconnect skeletal elements.

The unique structure of the daphniid carapace offers remarkable protection with minimal material investment. Our results provide a new mechanistic explanation for its high rigidity: using the hemolymphatic pressure as a supporting element, daphniids use a light-weight construction consisting of two integuments connected via flexible ligaments and inflated by a hemolymphatic hyper-pressure to protect their body from the

environment. Because hemolymph has a similar density to water, this construction does not impose negative effects on swimming. In conclusion this structure seems to be an excellent compromise between protection and swimming capability that may play an important role in *Daphnia* success in lentic ecosystems.

ACKNOWLEDGMENTS

We want to thank Prof. Dr. Jasna Štrus for valuable comments and ideas and Gabi Strieso, Ioanna Ioannidou, Sabine Adler and Tanja Rollnik for valuable contributions that greatly improved our procedures. We thank Thomas White for correction of the English language. Author Contributions: SK, MH, LCW and RT designed the study. SK and MH performed the experiments. LCW, SK and MH analyzed the data. SG and CS designed the experimental setup for the hemolymphatic pressure measurements and provided valuable ideas on the data interpretation. SK and LCW wrote the manuscript. All authors contributed to the final version of the manuscript.

LITERATURE CITED

Anderson BG. 1933. Regeneration in the carapace of *Daphnia magna*. Biol Bull 64:70–85.

Barry MJ. 2000. Inducible defences in *Daphnia*: Responses to two closely related predator species. Oecologia 124:396–401.

Bitsch C, Bitsch J. 2002. The endoskeletal structures in arthropods: Cytology, morphology and evolution. Arthropod Struct Dev 30:159–177.

Carbone G, Pierro E, Gorb SN. 2011. Origin of the superior adhesive performance of mushroom-shaped microstructured surfaces. Soft Matter 7:5545–5552.

Chen B, Yin D, Ye W, Lin S, Fan J, Gou J. 2015. Fiber-continuous panel-pillar structure in insect cuticle and biomimetic research. Mater Des 86:686–691.

Dodson SI. 1974. Adaptive change in plankton morphology in response to size-selective predation: A new hypothesis of cyclomorphosis. Limnol Oceanogr 19:721–729.

Fryer G. 1991. Functional morphology and the adaptive radiation of the Daphniidae (Branchiopoda: Anomopoda). Philos Trans R Soc Lond B Biol Sci 331:1–99.

Fryer G. 1996. The Carapace of the Branchiopod Crustacea. Philos Trans R Soc B Biol Sci 351:1703–1712.

Grant JWG, Bayly IA. 1981. Predator induction of crests in morphs of the *Daphnia carinata* King complex. Limnol Oceanogr 26:201–218.

Halcrow K. 1976. The fine structure of the carapace integument of *Daphnia magna* Straus (Crustacea: Branchiopoda). Cell Tissue Res 169:267–276.

Hebert PDN. 1977. A revision of the taxonomy of the gennus *Daphnia* (Crustacea: Daphnidae) in south-eastern Australia. Aust J Zool 25:371–398.

Heepe L, Gorb SN. 2012. Biologically inspired mushroom-shaped adhesive microstructures. Annu Rev Mater Res 44: 173–203.

Janmey PA. 1991. Mechanical properties of cytoskeletal polymers. Curr Opin Cell Biol 3:4–11.

Krueger DA, Dodson SI. 1981. Embryological induction and predation ecology in *Daphnia pulex*. Limnol Oceanogr 26: 219–223.

Laforsch C, Tollrian R. 2000. A new preparation technique of daphnids for scanning electron microscopy using hexamethyldisilazane. Arch für Hydrobiol 149:587–596.

Laforsch C, Ngwa W, Grill W, Tollrian R. 2004. An acoustic microscopy technique reveals hidden morphological defenses in *Daphnia*. Proc Natl Acad Sci USA 101:15911–15914.

Lampert W. 1989. The adaptive significance of diel vertical migration of zooplankton. Funct Ecol 3:21–27.

Leydig F. 1860. Naturgeschichte der Daphniden, Tübingen: Verlag der H. Laupp'schen Buchhandlung. 290 p.

Louette G, De Meester L. 2004. Rapid colonization of a newly created habitat by cladocerans and the initial build-up of a *Daphnia*-dominated community. Hydrobiologia 513:245–249.

Mattheck C. 1998. Design in Nature: Learning From Trees, 1st ed. Berlin: Springer Science & Business Media. 276 p.

Nardi JB, Ujhelyi E. 2001. Transformations of epithelial monolayers during wing development of *Manduca sexta*. Arthropod Struct Dev 30:145–157.

Olesen J. 2013. The crustacean carapace: Morphology, function, development, and phylogenetic history. In: Watling L, Thiel M, editors. Functional Morphology and Diversity. Oxford: Oxford University Press. pp 103–139.

Ottani V, Raspanti M, Ruggeri A. 2001. Collagen structure and functional implications. Micron 32:251–260.

Pirow R, Wollinger F, Paul RJ. 1999a. The sites of respiratory gas exchange in the planktonic crustacean *Daphnia magna*: An in vivo study employing blood haemoglobin as an internal oxygen probe. J Exp Biol 202:3089–3099.

Pirow R, Wollinger F, Paul RJ. 1999b. The importance of feeding current for oxygen uptake in the water flea *Daphnia magna*. J Exp Biol 202:553–562.

Schultz TW, Kennedy JR. 1977. Analyses of the integument and muscle attachment in *Daphnia pulex*. J Submicrosc Cytol 9:37–51.

Stevenson RJ. 1985. Dynamics of the integument. In: Bliss DE, Mantel LH, editors. The Biology of Crustacea Vol.9: Integument, Pigments, and Hormonal Processes. New York: Academic Press. pp 1–31.

Stibor H. 1992. Predator induced life-history shifts in a freshwater cladoceran. Oecologia 92:162–165.

Stibor H, Lüning J. 1994. Predator-induced phenotypic variation in the pattern of growth and reproduction in *Daphnia hyalina* (Crustacea: Cladocera). Funct Ecol 8:97–101.

Taylor BE, Gabriel W. 1992. To grow or not to grow: Optimal resource allocation for *Daphnia*. Am Nat 139:248–266.

Tollrian R. 1994. Fish-kairomone induced morphological changes in *Daphnia lumholtzi* (Sars). Arch für Hydrobiol 130: 69–75.

Tollrian R, Dodson SI. 1999. Inducible defenses in Cladocera: Constraints, costs, and multipredator environments. In: Tollrian R, Harvell CD, editors. The Ecology and Evolution of Inducible Defenses. Princeton, New Jersey: Princeton University Press. pp 177–202.

Weiss LC, Tollrian R, Herbert Z, Laforsch C. 2012. Morphology of the Daphnia nervous system: a comparative study on Daphnia pulex, Daphnia lumholtzi, and Daphnia longicephala. J Morphol 273:1392–1405.

Znidaršič N, Mrak P, Tušek-Žnidarič M, Strus J. 2012. Exoskeleton anchoring to tendon cells and muscles in molting isopod crustaceans. Zookeys 176:39–53.